Characteristics of strong ground motions recorded during the April 2009 L'Aquila (central Italy) seismic sequence

G. Ameri[1], M.Massa[1], D. Bindi[1], E. D'Alema[1], A. Gorini[2], L. Luzi[1], S. Marzorati[1], F.Pacor[1], R. Paolucci[3], R.Puglia[1] and C.Smerzini[4]
[1] Istituto Nazionale di Geofisica e Vulcanologia, Milan, ameri@mi.ingv.it
[2] Dipartimento della Protezione Civile - Ufficio Valutazione, Prevenzione e Mitigazione del Rischio Sismico (SISM), Rome
[3] Department of Structural Engineering, Politecnico di Milano, Milan
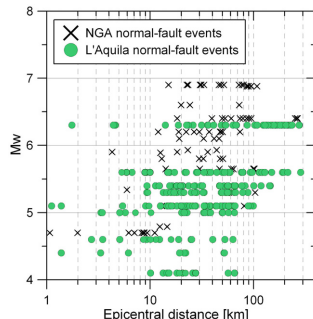[4] Rose School, Pavia

Strong-motion data set

The data set consists of about 300 strong motion data, recorded by the RAN and by the INGV MI-PV temporary network (http://rais.mi.ingv.it/).
The data can be downloaded from ITACA database (http://itaca.mi.ingv.it/)
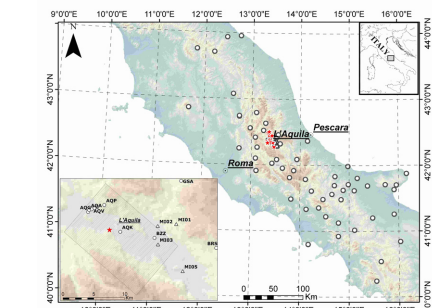
ABSTRACT
The 6 April 2009 L'Aquila MW 6.3 earthquake and its aftershocks yielded the most extensive set of strong-motion data in the near-source region yet obtained in Italy. The mainshock was recorded by 56 strong-motion stations belonging to the RAN, with 19 of these located within 50 km of the surface projection of the fault. The available data set is composed of more than 300 three-components strong-motion records from Mw ≥ 4 events recorded by RAN and INGV MI-PV stations, with about 90 records within 50 km of the corresponding epicenters. The strong ground motions from the mainshock show a clear dependence on azimuth, that can be attributed both to source effects (i.e., directivity effects) and to different attenuation properties of seismic waves at crustal scale (as suggested by the peak acceleration maps from the two strongest aftershocks). These records contribute to fill important gaps in the magnitude-distance-style of faulting distributions of global and regional data sets used to derive ground motion prediction equations. The near-fault ground motions (R$_{JB}$=0) are generally underestimated by GMPEs, while at larger distances the opposite trend is observed, especially for high-frequency ground motion parameters (i.e., PGA). The residuals calculated for the whole sequence respect to different GMPEs show a negative bias indicating that the recorded ground motions are on average smaller than the ones predicted the empirical models. Preliminary analysis of near-fault records from the mainshock shows that peak motion varies significantly for stations within 5 km from the epicenter. The PGA ranges from 327 to 646 cm/s² (not considering the AQM saturated station). A specific baseline correction procedure was applied to these records in order to recover permanent displacements, that were found to be consistent with results based on GPS measurements. A comparison of the observed acceleration response spectra with recently proposed design spectra for the town of L'Aquila shows that the near-fault motion generally exceeded the no-collapse limit state design spectra both for horizontal and vertical components.

Fig.1 - Location of the accelerometric stations belonging to RAN (circles) and to INGV MI-PV (triangles). The red star denotes the epicenters of the 13 events with M$_W$ ≥ 4. In the inset the surface projection of the fault and the mainshock epicenter are shown.


The L'Aquila data set is of major relevance for a complex regional context such as Italy, as well as worldwide, as normal-fault events are poorly represented in global strong-motion databases. **Fig. 2** – Magnitude vs. distance distribution of the data from normal-fault events recorded during the L'Aquila sequence for Mw> 4.0 by RAN and INGV MI-PV stations (gray dots) compared to those listed in the NGA database, Chiou et al.,2008 (black crosses).
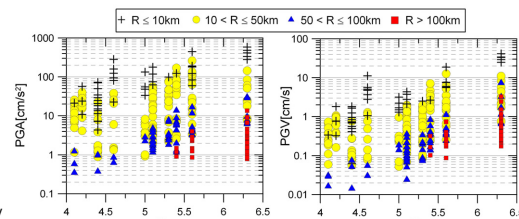
Fig. 3 – Geometric mean between horizontal components of PGA (left) and PGV (right) from the largest earthquakes (M$_W$ ≥ 4) of the L'Aquila seismic sequence, plotted as a function of Moment Magnitude. The different symbols indicate different epicentral distance ranges.

Spatial distribution of ground motion

MAINSHOCK
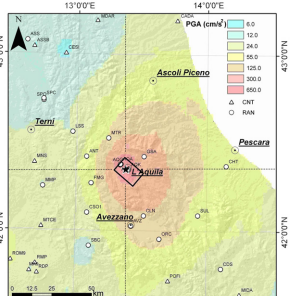
Fig. 4 – upper panel: Peak ground acceleration map (maximum horizontal component) for the mainshock obtained interpolating data from different seismic networks (triangles: National Seismometric Network, INGV-CNT; dots: Italian Strong-Motion Network, RAN). The northeast, southeast, southwest and northwest quadrants, with respect to the epicenter, are highlighted.
Lower panel: Residuals of acceleration spectral ordinates (5% damping), at periods of 0.3 (red dots) and 2.0 (black crosses) seconds, calculated respect to the ITA08 ground motion prediction equations (Bindi et al., 2009). Residuals are plotted versus the source-to-station azimuth measured clockwise from north for RAN stations within 100km. Vertical lines show the fault strike and up-dip directions (147° and 57°, respectively). Note that residuals having R$_{JB}$=0 are plotted as gray symbols. We restricted the analysis to data from RAN stations within 100km of the fault.
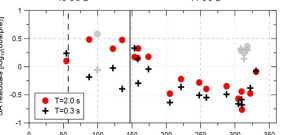
LARGEST AFTERSHOCKS
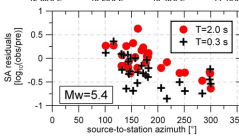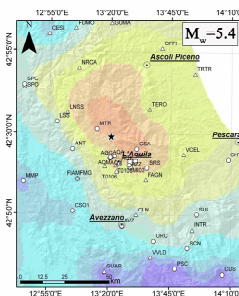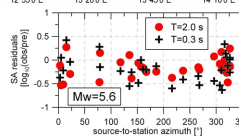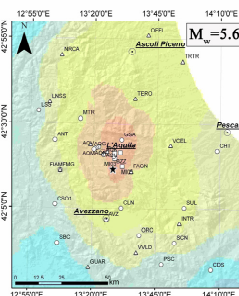
Fig.5 – The same as Fig. 4 but for the April 7, M$_w$ 5.6 and April 9, M$_w$ 5.4, events. PGA maps (maximum horizontal component) are obtained interpolating data from different seismic networks (triangles: INGV-CNT; squares: temporary strong-motion stations, INGV MI-PV; dots: RAN).

The residual distribution in **Fig.4** shows a clear trend with azimuth: at long periods (T=2.0 s), observations in the northeast and southeast quadrants (stations with azimuths from about 50° to 180°) are underestimated by the ITA08 model (positive residuals) while those in the western quadrants (from 200° to 330°) are overestimated (negative residuals). Because the fault strike and up-dip directions (147° and 57°, respectively, shown by vertical lines in Fig.4 lower panel) point towards the southeast and northeast quadrants, the positive residuals for long-period motions can be explained as directivity-induced amplification effects due to both up-dip and along-strike rupture propagation (e.g., Aagaard et al., 2004). The negative residuals obtained at short and long periods in the northwest and southwest quadrants (200°-to-330° azimuth range) can be both ascribed to backward directivity effects and to different seismic wave attenuation with respect to the eastern sector. This latter explanation seems supported by **Fig.5** where the faster decay of ground motion amplitude toward W-SW is visible in the PGA maps of the two largest aftershocks. Moreover the residual distributions show that the observed spectral values are overestimated by the ITA08 model at both short and long periods for sites located W-SW of the relative epicenters.

Comparison with Ground Motion Prediction Equations

We compare the attenuation with distance of the peak ground motion parameters, (PGA and PGV), observed during the mainshock, with predictions from global and regional models: Bindi et al. (2009, ITA08), developed for Italy, Akkar and Bommer (2007a,b; AkB07), based on the European and Middle East data, and Boore and Atkinson (2008, BAT08), calibrated with worldwide data set.
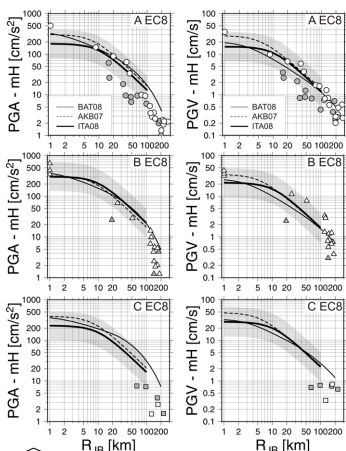

Fig.6 - Peak ground acceleration (PGA) and velocity (PGV) for the mainshock (maximum horizontal component, mH) versus Joyner and Boore distance (R$_{JB}$). Data are separated according to EC8 site classification and compared with different ground motion prediction equations. Empty and gray filled symbols correspond to observations over the azimuthal range 0° - 180° and 180° - 360°, respectively. The shaded area represents the mean plus and minus one standard deviation interval of the ITA08 GMPE. Note that points with RJB less than 1 km are plotted at 1 km as empty symbols.
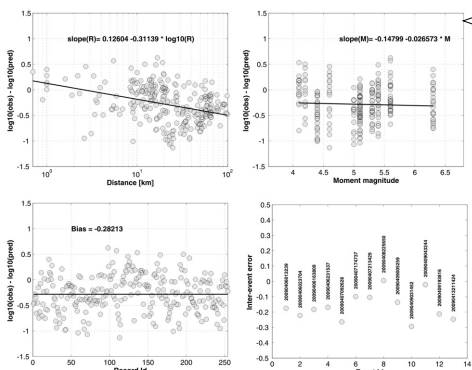
Fig.7 – PGA residuals calculated for the L'Aquila sequence (13 events with M$_W$≥4) respect to the ITA08 GMPE. Residuals are plotted as a function of distance, magnitude and record. The lower-left plot shows the inter-event errors (i.e., mean of the residuals for each event).

The comparison (**Fig.6**) with GMPEs considering PGA and PGV up to 100 km confirms the azimuthal dependence shown in Fig.4. In particular, for distances from 10 to about 100 km and for all site classes, the data east to the epicenter (azimuth 0° - 180°) follow the median trend estimated by the GMPEs, while the sites located in the western sectors (180° to 360°) are less than the median minus one standard deviation. At distances larger than 100 km PGAs show a faster decay than PGVs. Moreover the azimuth dependence is not clearly evident as for shorter distances. The near-fault PGAs and PGVs (R$_{JB}$ = 0 km) are underestimated by mean predictions but in general are within one standard deviation of the empirical models.
The residuals calculated for the whole sequence (**Fig.7**) show significant dependence on distance (resulting from the data beyond 25 km) while no dependence on magnitude is found. Finally, the negative bias indicates that the recorded ground motions are on average smaller than the ones predicted the GMPE.

Near-fault records

The stations of the Aterno Valley array are located within the surface projection of the L'Aquila mainshock fault and are at distances less than 5 km from the mainshock epicenter (Fig. 1). This array, together with the AQK station located close to L'Aquila downtown, provided a near-fault strong-motion data set, never recorded in Italy for any event with M > 5.
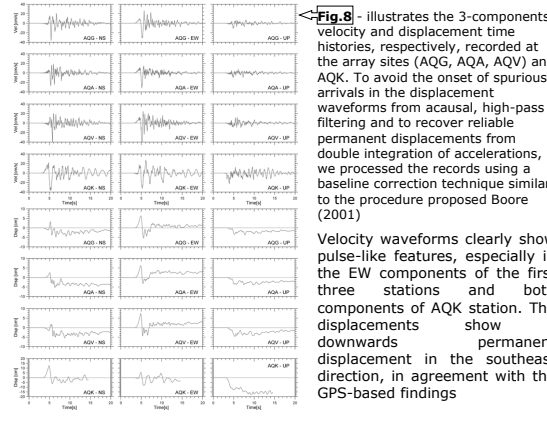
Fig.8 - illustrates the 3-components velocity and displacement time histories, respectively, recorded at the array sites (AQG, AQA, AQV) and AQK. To avoid the onset of spurious arrivals in the displacement waveforms from acausal, high-pass filtering and to recover reliable permanent displacements from double integration of accelerations, we processed the records using a baseline correction technique similar to the procedure proposed Boore (2001)

Velocity waveforms clearly show pulse-like features, especially in the EW components of the first three stations and both components of AQK station. The displacements show a downwards permanent displacement in the southeast direction, in agreement with the GPS-based findings

References
-Aagaard, B.T., Hall, J.F. and T.H. Heaton (2004). Effects of fault dip and slip rake angles on near-source ground motions: why rupture directivity was minimal in the 1999 Chi-Chi, Taiwan, earthquake, *Bull. Seism. Soc. Am.*, 94, 155-170.
-Akkar S. and J.J. Bommer (2007a). Empirical prediction equations for peak ground velocity derived from strong-motion records from Europe and the Middle East, Bull. Seism. Soc. Am., 97 (2), 511-530.
-Akkar S. and J.J. Bommer (2007b). Prediction of elastic displacement response spectra in Europe and the Middle East, Earthquake Eng. and Struc. Dyn., 36, 1275-1301.
-Boore D.M. (2001). Effect of baseline corrections on displacements and response spectra for several recordings of the 1999 Chi-Chi, Taiwan, Earthquake. Bull. Seism. Soc. Am., 91, 1199-1211.
-Boore D.M. and G.M. Atkinson (2008). Ground motion prediction equations for the mean horizontal component of PGA, PGV and 5%-damped PSA at spectral periods between 0.01 s and 10.0 s, Earthquake Spectra, 24, 1, 99-138.
-Chiou B., Darragh R., Gregor N. and W. Silva (2008). NGA project strong-motion database, Earthquake Spectra, 24, 23-44.